In presenting the dissertation as a partial fulfillment of the requirements for an advanced degree from the Georgia Institute of Technology, I agree that the Library of the Institute shall make it available for inspection and circulation in accordance with its regulations governing materials of this type. I agree that permission to copy from, or to publish from, this dissertation may be granted by the professor under whose direction it was written, or, in his absence, by the Dean of the Graduate Division when such copying or publication is solely for scholarly purposes and does not involve potential financial gain. It is understood that any copying from, or publication of, this dissertation which involves potential financial gain will not be allowed without written permission.

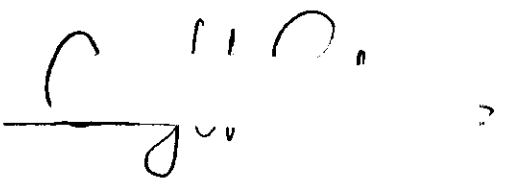

7/25/68

THE RELATIVE POPULATION DISTRIBUTION OF THE VIBRATIONAL QUANTUM LEVELS OF $N_2^+ B^2\Sigma_u$ RESULTING FROM COLLISION BETWEEN Ne^+ AND N_2

A THESIS

Presented to

The Faculty of the Graduate Division

by

Gary H. Saban

In Partial Fulfillment

of the Requirements for the Degree

Master of Science in Chemistry

Georgia Institute of Technology

March, 1972

THE RELATIVE POPULATION DISTRIBUTION OF THE VIBRATIONAL QUANTUM LEVELS OF $N_2^+ B^2\Sigma_u$ RESULTING FROM COLLISION BETWEEN Ne^+ AND N_2

Approved:

Chairman

Date approved by Chairman: 2/22/72

ACKNOWLEDGMENTS

It is with sincere appreciation that I acknowledge the invaluable and understanding assistance of my research advisor, Dr. Thomas F. Moran, in the construction of the apparatus, acquisition and interpretation of the data, and in the preparation of this manuscript. I am also grateful to Dr. Raymond F. Borkman and Dr. Sidney L. Gordon who served as my reading committee.

Additionally, I am indebted to the United States Air Force Institute of Technology and Dr. William M. Spicer for having afforded me the opportunity to attend the Georgia Institute of Technology in pursuance of the degree, Master of Science in Chemistry.

TABLE OF CONTENTS

TABLE OF CONTENTS (Concluded)

LIST OF TABLES

LIST OF ILLUSTRATIONS

SUMMARY

A crossed ion beam-molecular beam apparatus was built and used to study a low energy electron transfer reaction. The system selected was the ion molecule collision reaction between Ne^+ and N_2 which provides an experimental test of the mechanism of energy conversion in an exothermic reaction at high reactant ion velocities. This was a convenient system for analysis because (1) the excited B state of N_2^+ is extremely short lived (undergoing spontaneous radiative transitions prior to leaving the collision area) and (2) the emission from this transition occurred in a convenient portion of the spectrum. This second reason was extremely important in that it greatly simplified the collection of data.

The collision species, Ne^+, was generated by electron bombardment of neon. These ions were then drawn away from their place of generation by a series of accelerating plates. They were then focused and brought into collision with a beam of neutral nitrogen molecules. The velocity component of the nitrogen was normal to the path of the Ne^+ ions.

Some of the excited reaction products underwent a spontaneous radiative transition in 10^{-8} seconds. (This was rapid when compared to the time required for the reactants to pass through the collision region.) The transition of excited N_2^+ ($B^2\Sigma_u^+$) to the ground state ($X^2\Sigma_g^+$) resulted in the emission of radiation in the ultraviolet through visible regions of the spectrum. Analysis of the emission spectra led to deductions regarding (1) the kinetic energy dependency of the reaction cross section

and (2) the nature of the relative population distributions of the vibrational quantum levels of the excited N_2^+ species in the B^{2+} state.

CHAPTER I

INTRODUCTION

Previous Work

Effort has been expended in determining the mechanism of reactions of the type

$$A^+ + B \rightarrow A + B^+_{excited}$$

$$B^+_{excited} \rightarrow B^+ + h\nu$$

where the reaction is spontaneously radiative, and $h\nu$ is in the visible region of the electromagnetic spectrum.

Past experiments show that, for the collision between Ne^+ and the noble gases, the cross sections for the charge transfer with optical excitation are of the same order of magnitude as for the total charge transfer (1,2,3). In this connection, it is significant that the optical excitation is possible either through conversion of a part of the kinetic energy of the colliding ion into internal energy or from the heat evolved due to the reactions exoergicity. Early studies of optical excitation by ion impact at higher energies have not revealed the mechanism of reaction at the lower energies (4). Lipiles and co-workers (2) believe that the excitation involves a molecular-ion complex formed during collision. According to Massey, a system will have a maximum probability (to the first approximation) for transition in a collision when the following

equality is satisfied (5).

$$\left(\frac{\Delta E}{h}\right)\left(\frac{b}{v_m}\right) \cong 1 \qquad (1)$$

Here, ΔE is the difference in internal energy between the two states of the system, b is the impact parameter, and v_m is the relative velocity of the colliding particles. It can be seen that the probability for excitation decreases very rapidly as the velocity is made smaller than v_m. According to experiments by Schlumbohm (6), the cross section for Ne^+ on N_2 is about 2×10^{-18} cm^2, or an impact parameter of about 6×10^{-9} cm. Using 10 eV as an approximate value for ΔE, the corresponding velocity for maximum cross section would be for a 1 keV ion. On this basis, a very small cross section should be expected at low energies. However, Lipeles points out that, although arguments of this type have generally been used to indicate that optical excitation with ions can only occur at relatively high energies, such a conclusion is contrary to work accomplished by his group (2). By the application of a molecule-ion complex intermediate, Lipeles' work can be reconciled with the predictions of equation (1) (2,33).

The Schlumbohm work previously referenced was concerned with the experimental investigation of optical excitations in collisions of Ne^+ ions with the molecules N_2, O_2, and CO_2 (for collision energies between 2 and 250 eVolts). The work concludes that the reaction cross section is kinetic energy dependent. This is basically in agreement with Gustafsson and Lindholm (7) in that Schlumbohm's data can be normalized to Gustafsson and Lindholm's data for kinetic energies above 150 eVolts.

The work also shows that the spectrum is due to emission from the excited molecular N_2^+ species and that many vibrational levels above v=0 are populated.

Purpose

Of the many questions remaining unanswered with respect to the light emission from charge transfer type reactions, the ones with which this thesis will concern itself are (1) clues to the nature of the kinetic energy dependency of the reaction cross section and (2) the relative population distribution of the vibrational quantum levels of excited N_2^+ in the $B^2\Sigma_u^+$ state. This will be for the kinetic energy range of 50 to 450 eVolts.

Such information is essential for future elucidation of the reaction mechanism between the above energy limits.

CHAPTER II

APPARATUS

Introduction

The experimental apparatus consisted primarily of a double beam ion molecular collision chamber coupled to electronic devices capable of measuring electromagnetic radiation in the near ultraviolet through the low visible wave length spectra. A total of seven pumps were used to maintain an operating pressure of about 10^{-3} - 10^{-4} torr. The primary ion beam was produced by electron impact in the source. Ions exiting the source were electrostatically focused, energetically controlled between 10 and 450 eVolts, and propelled into a neutral beam of nitrogen injected normal to the path of the ions. The charge transfer and spontaneous radiative transitions of the excited N_2^+ species both took place in field free space (see Figure 1). The above experimental conditions insured only single collisions occurred. Analysis of the light emitted was made using photomultiplying circuits. All electronic and glass connections entering the evacuated chamber were made through a 25.4 mm aluminum flange bolted to the end of the main portion of the vacuum chamber. Each of the two gas systems was externally controlled. The entire experiment was enclosed in a protective light tight structure which helped eliminate stray photons from entering the apparatus and counting circuits. A more detailed description of the construction and operation of the individual components will follow.

Ion Source

The primary ion beam, Ne^+, was generated in a gas phase electron impact source constructed of polished 304 stainless steel. Pyrex glass spacers were used for electrical insulation, separation between accelerating plates, and alignment of the focusing plate. The source, with its plates, was rigidly supported by four stainless steel rods insulated in the same manner as described above. Schematic diagrams of the source assembly are shown in Figure 1. The ionization chamber itself was cylindrical and measured 15.88 mm long by 25.40 mm in diameter. Electrons were boiled off a directly heated carborized rhenium filament through a 3.18 mm diameter hole (electron inlet hole) perpendicular to the axis of the ionization chamber. These electrons were then collected on the opposite side of the ionization chamber by a trap. The filament, a 20 mm long piece of .127 mm diameter wire, was bent into the shape indicated in Figure 1 and suspended above the electron inlet hole by specially designed mounts. The area was then covered by a 304 stainless steel housing maintained at the same potential as the filament. This housing also served as a shield in preventing visible light radiated by the flowing filament during operation from being internally reflected through the apparatus and into the photomultiplying circuits. The filament was heated by directly passing 5 to 7 amperes through it. This gave a trap current of approximately 11 ma. Electron emission was regulated by the filament power supply to $\pm$ 0.1 μa by a trap current feedback loop. The filament, trap, and repeller were floated from the ionization chamber potential by the filament power supply. To prevent reflection of electrons of unknown

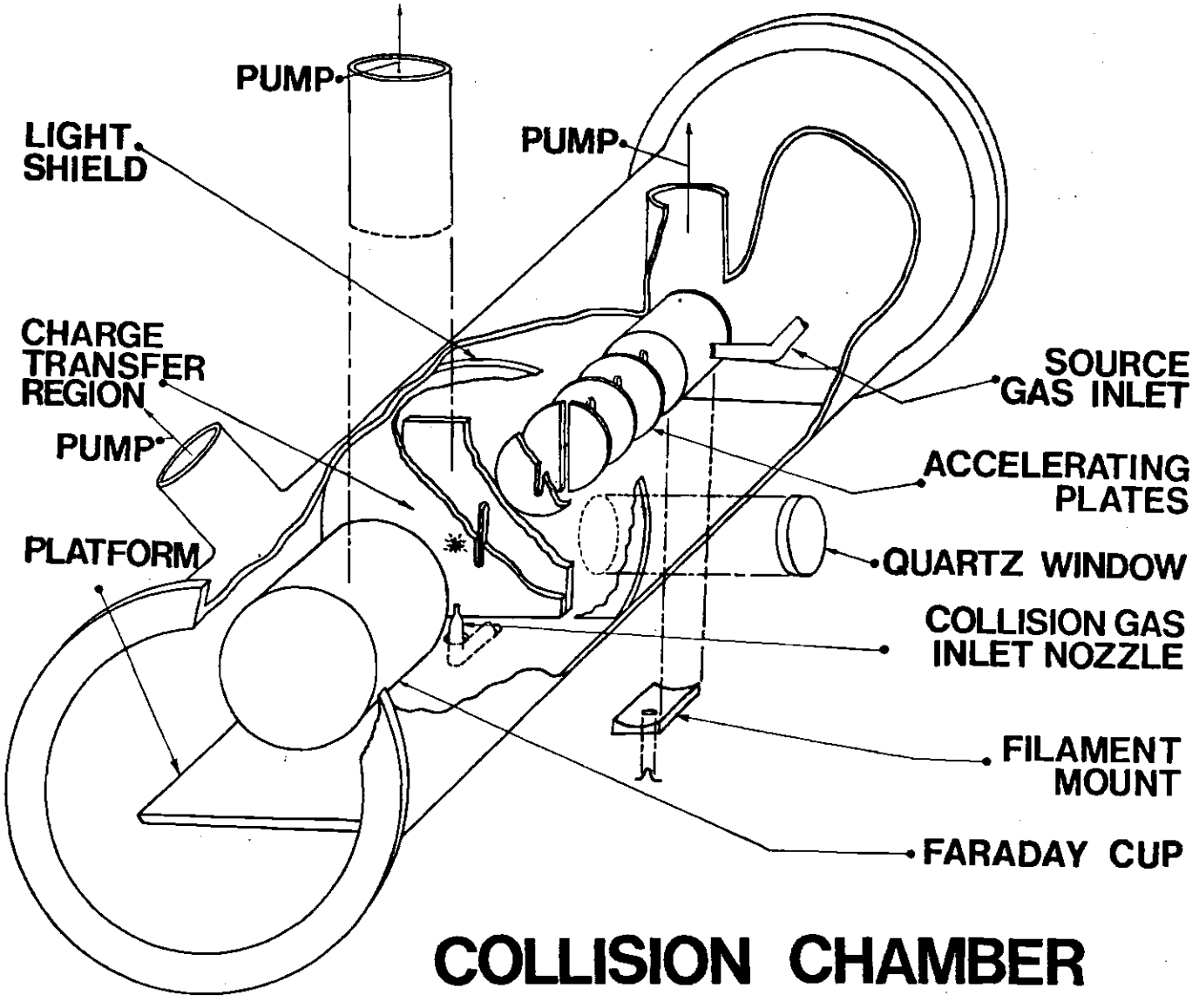

Figure 1. Collision Chamber

energy back into the ionization region, the trap was shielded by a stainless steel plate containing a 5 mm diameter hole for the passage of electrons. The primary gas inlet port was perpendicular both to the axis of the chamber and to the electron beam. The glass to metal connection was via a 3.00 mm ID Kovar seal attached directly to the stainless steel ionization chamber of the source. The electron beam impinged on the ion source gas which was then ionized. The ions were then forced out of the chamber through a 3.18 X 15.88 mm slit by a repeller plate located inside the source.

The ion accelerating system consisted of four accelerating plates. Each was 0.922 mm thick and spaced 2.74 mm apart. The first three plates were used strictly as accelerating plates. The fourth was vertically split and could be used for focusing to compensate for beam expansion. High voltage for the ionization chamber and accelerating plates was supplied via a unit designed specifically for this experiment. Voltages were individually controllable. The range of available voltages is given in Table 1. The source itself was continually variable from 0 to 450 volts.

Table 1. Measured Range of Individually Controllable Plate Voltages in the Source

System	Voltage Range	
	Min	Max
Source	0	450
A1	0	145
A2	0	144
A3	0	148
Focus Left	0	139
Focus Right	0	139

Support Electronics

With the target gas off, the primary ion beam intensity was measured using a Faraday cup located aft of the collision region and on the same axis as the source ion exit port and accelerating/focusing plates. Measurements were made using a Keithley high speed picoammeter (model 417). Both the source and Faraday cup were mounted on a 50 mm x 90 mm x 485 mm aluminum plate which was set inside the chamber in such a position that the collision region was perpendicular to a quartz window. Typical operating primary ion beam intensities were about 10^{-8} amps. Internal pressure during experimentation was monitored using a Consolidated discharge vacuum gauge. The method is discussed in Chapter III.

Gas Inlet Systems

Both the primary ion beam source gas and the collision gas were introduced into the collision chamber from high purity high pressure Matheson cylinders. Each gas flowed from the cylinder through its own pressure reducing two stage regulator, an Edwards fine control needle valve (model LB2B), a stopcock, and into 14 mm glass tubing. The glass tubing transited the flange and was connected to Tygon inside the chamber. The neon then entered the source through a Kovar connector while the nitrogen was jetted into the impact area through a converging-diverging glass nozzle mounted normal to the path of the ions.

Vacuum System

Four diffusion pumps were used to maintain operating pressure: two National Research Corporation water cooled silicon oil diffusion pumps (each rated at 150 liters per second) and two mercury diffusion pumps

(each rated at 300 liters per second).* Whenever the system was in operation below 10^{-3} torr, the mercury diffusion pump traps were filled with powdered dry ice.

The system was evacuated from four locations. See Figure 1. Two 65 mm glass pipes connected to the ballast setting directly over the collision region provided the majority of the pumping. Two other 65 mm pipes were connected directly to the main portion of the collision chamber; one aft of the Faraday cup, one forward of the source. When the system was to be evacuated, the mechanical roughing pumps were started. At approximately 1 torr, the four diffusion pumps were started and all seven pumps operated until high vacuum was achieved. Several days were usually required whenever the system had been exposed to the atmosphere. All pumps ran continuously during experimentation. Electrical power to each pump was individually controlled. If necessary, the system could be vented without disconnecting any of the pumps or gas inlet devices.

Access to the inside of the tank was through two removable 270 x 6 mm circular aluminum flanges bolted to each end of the cylindrical collision chamber. A large rubber "O" ring was fitted between the flange and the ground glass end plate of the tank which insured a vacuum tight connection. All leads into the tank passed through one of the flanges. The electrical connector leads at the flange were 3KVA Ceramaseal High Vac electrical feedthroughs and the gas leads were 14 mm glass tubing.

---

*The mercury pumps were manufactured by the Georgia Institute of Technology glass blowing shop.

Photon Collection

As collision took place between the ion beam and the neutral gas, a certain amount of the reactants underwent a charge transfer reaction leading to $N_2^+B^2\Sigma_u^+$. In accordance with the kinematics and dynamics to be discussed in Chapter V, the excited $N_2^+B^2\Sigma_u^+$ species will undergo spontaneous radiative transition. Emission of photons will take about 10^{-8} seconds. As the photons radiated omnidirectionally, a portion passed through the quartz window mounted into the side of the collision chamber. They were then collected by an EMI 6256S photomultiplier with a flat spectral response in the region of interest. The photomultiplier was connected to an Ortec preamplifier, amplifier, shaper, timer, and counter. The output from the Ortec electronics was read and recorded.

Special Shielding

As the heated filament radiated extremely high numbers of photons when compared to those due to collision of the reactants, prevention of stray light entering the photomultiplier was imperative. Accordingly, a series of flutes, baffles, and barriers coated with Aquadag (a paint consisting of a colloidal suspension of graphite in an aqueous base) was strategically arranged to prevent unwanted light originating from filament glow. The entire apparatus was also enclosed in a three quarter inch thick metal and wood housing. This housing reduced the amount of unwanted light from sources other than the filament light as well as acting as a protective shield for the system operator.

Safety

Extreme care was used in design considerations and construction with operator safety being of paramount importance. All high voltage and current using electronic components were separately fused. A relay system prevented the diffusion pumps from operating above 1 torr. This was necessary since the system continued to pump 24 hours a day. In the event of system failure, all electronics were immediately isolated from the collision apparatus. Critical controls could not be operated without special devices. Also, the entire chamber was always kept inside a protective housing to prevent personal injury in the event of an accidental explosion or implosion of the glass vacuum system. Fortunately, no part of the system concerned with operator safety failed during the entire experiment.

CHAPTER III

EXPERIMENTAL PROCEDURES

General

The experimental apparatus and general conditions used to conduct this series of experiments were presented in Chapter II. Before meaningful data could be collected, however, two determinations unique to double beam collision experiments using glowing filaments as an electron generator had to be made. These were the experimental determination of (1) the effect of a repeller plate in the source on the kinetic energy distribution of the ejected ions and (2) the optimum internal shielding and surface coatings required to minimize electronic photomultiplier noise generated by the glowing filament. Results led to the reaction cross sections' kinetic energy dependency and the probable vibrational population distributions at several kinetic energies.

Repeller Correction

Since a repeller was used to eject the Ne^+ ions from the source, the kinetic energy of the ions was higher than expected from the voltage difference between the source potential and ground. With an applied ion repeller voltage, the source chamber is not an equipotential volume and ions exit the source with a kinetic energy proportional to the repeller voltage. This proportionality constant can be determined using standard techniques (8). The energy of the electron beam is also increased by the

repeller potential as it enters the ionization chamber and results in an apparent lowering of the ionization potential of the neutral gas target from its spectroscopic value. This measured energy difference, between spectroscopic and experimental ionization potentials, can be used to obtain the repeller contribution to the ion kinetic energy. It was found that the ions exited the source with 0.44 eVolts per applied repeller volt.

Internal Shielding

When current in sufficient amounts to cause electron emission is passed through the filament, the filament glows white hot, acts as a black body radiator, and floods the visible spectrum in the same vicinity where the spontaneous radiative transitions to be studied take place. The necessity to prevent great numbers of photons from the filament from entering the counting circuitry is of paramount importance. Failure to properly do so results in electronic noise and causes a reduction in the signal to noise ratio. Too low a ratio would have prevented collection of useful data.

A series of flutes, baffles, and barriers coated with Aquadag was continually rearranged until optimum shielding was achieved. Verification of such was demonstrated by placing a strip of Kodac type 103A F spectroscopic safety film over the quartz window and exposing it for 24 hours using different internal shielding and surface coatings. The filament was operated at the intended experimental temperatures. The final arrangement with the Aquadag coating produced no significant film exposure. Also, there was no appreciable increase in the noise level recorded (in the ab-

sence of reactants) when the cold filament was compared to the emitting or hot filament.

Cross Section Kinetic Energy Dependence

The ionic species Ne^+ was generated in the source by electron bombardment of neon (Matheson Research Grade, the only impurity being helium in abundance of 12 ppm). The ions were ejected from the source by the repeller plate set at a specific potential. Once clear of the source, the ions were accelerated through a series of charged plates, a collision region, and into a Faraday cup where they were collected. The current generated was recorded. This measurement was later used to normalize data collected at different primary ion beam currents. Typical recorded values ranged from 10^{-8} to 10^{-9} amperes.

Incident to the path of the primary ion beam, the neutral collision species N_2 was injected so that collisions would take place. The collision gas N_2 was Matheson Prepurified Grade, 99.9 percent minimum N_2. Operating pressures were regulated by first measuring system pressure without gas flow, then with just the ion source gas, and finally with both the ion source gas and the collision gas. By this method, it was unnecessary to rely on readings from the series of pressure reducing devices in order to determine exact operating partial pressures of the gaseous reactants. All pressures were recorded during each experiment and used in the compilation of data.

As collision and reaction took place, a portion of the omnidirectionally generated radiation passed first through a quartz window, then through interchangeable optical filters, and finally into a photomultiplier

tube. The amount of radiation generated was recorded. The modus operendi was generally to start at minimum source potential and, using a given repeller voltage, maximize primary ion beam current, allow system stabilization, and record all pertinent readings. Source potential was then increased with the above process repeated until an entire scan of all available kinetic energies was made in both the increasing and decreasing directions. The "reversing" was so that any abnormal (9) conditions attributable to phenomena such as space charge, electronic drift, etc. would be detected. There were none. All data necessary for the determination of the reaction cross sections' kinetic energy dependence were now available.

Probable Vibrational Distributions

The previous experimental procedures were then repeated holding the source potential constant and changing the glass optical filter located between the quartz window and the photomultiplier tube. Comparative data were then collected. The three filters used were the Corning CS 7-60, Corning CS 7-51, and the Bausch and Lomb 33-78-39. The filters were then placed in a Cary 14 where their percent absorbance was measured in the spectral region concerned. With additional information obtainable from current literature (10,11,12), the probable relative vibrational population distributions could be determined.

CHAPTER IV

RESULTS

Introduction

We are basically concerned with the transition probabilities in the first negative band in the N_2^+ system. The probability of a transition from one vibrational level in an electronic state to another vibrational level can be expressed as the total eigenfunctions for the two states. Letting

v' = initial vibrational level

v'' = final vibrational level

i = initial electronic state

j = final electronic state

ψ_i = eigenfunction of initial state

ψ_j = eigenfunction of final state

$\mathcal{M}_e$ = electronic dipole moment operator

the probability (P) for the transition can be written as

$$P_{iv',jv''} \sim \left| \int \psi_{iv'}^{*} \mathcal{M} \psi_{jv''} d\tau \right|^2 \qquad (2)$$

where the integral is taken over the configuration space, τ (12). Herzberg has shown that the total eigenfunction of the state can be written as the product of the electronic and vibrational eigenfunctions

(ψ_e and ψ_v) neglecting the rotation of the molecule (13). Within the framework of the Born-Oppenheimer approximation, it can be assumed that the nuclear motion is separable from the electron motion. Therefore, letting R equal the internuclear distance and R^e_{ij} equal the electronic dipole moment from i to j, expression (2) can be reduced to

$$P_{iv',jv''} \sim \left|\iint \psi_{v'}\psi_{v''}\mathcal{M}_e\psi_{e'}{}^*\psi_{e''}dRd\tau_e\right|^2 \tag{3}$$

The integral over the vibrational wave functions (which depends only on R) is the "Franck-Condon factor" (also referred to as the square of the overlap integral). The second integral in expression (3) is R^e_{ij}. Note that it is taken over the volume space of the electron coordinates.

$$R^e_{ij} = \int \mathcal{M}_e\psi_{e'}\psi_{e''}d\tau_e \tag{4}$$

The electronic transition moment, R^e_{ij}, will, to a first approximation, vary slowly with R. Therefore, we can replace R^e_{ij} with an average value, $\overline{R^e_{ij}}$. Expression (3) now reduces to

$$P_{iv',jv''} \sim \left(\overline{R^e_{ij}}\right)^2\left|\int \psi_{v'}\psi_{v''}dR\right|^2 \tag{5}$$

or more simply,

$$\text{Probability} \sim (\text{Franck-Condon Factor})^2\left(\begin{matrix}\text{Average Electronic}\\ \text{Transitron Moment}\end{matrix}\right)^2 .$$

The intensity, I, of an emission of the type dealt with here is defined as the number of photons emitted by the collision source (or the point of reaction) per second. The first negative band of the N_2^+ emission spectrum deals with many different vibrational transitions between the $B^2\Sigma_u^+$ and $X^2\Sigma_g^+$ electronic states. The intensity of the emission in photons per second is given by the relation:

$$I_{v'v''} \sim N_{v'}(E_{v'v''})^3\left(\overline{R^e_{ij}}\right)^2\left|\int \psi_{v'}\psi_{v''}dR\right|^2 \tag{6}$$

The term $N_{v'}$ is the population of the v' level and $E_{v'v''}$ is the energy quantum required for the v'→v'' transition. Inclusion of the constant C, which is dependent on the experimental geometry, allows for simplifying expression (6) to the following equality,

$$I_{v'v''} = C(N_{v'})(E_{v'v''})^3(P_{iv',jv''}) \tag{7}$$

Because the average electronic transition moment, $\overline{R^e_{ij}}$, is assumed not to vary with a v'→v'' transition in a given band, the ratio of I of any two lines will be as the frequency of the emissions cubed times the ratio of the Franck-Condon factors of the transitions times the ratio of the relative vibrational populations. Since E is proportional to the wave number ω_e,

$$\text{Ratio} = \frac{I_{v'v''}}{I_{v''v'''}} = \frac{CN_{v'}(E_{v'v''})^3P_{iv',jv''}}{CN_{v''}(E_{v''v'''})^3P_{iv'',jv'''}} \tag{8}$$

or,

$$\text{Ratio} = \frac{N_{v'}}{N_{v''}} \left(\frac{\omega_{ev'v''}}{\omega_{ev''v'''}}\right)^3 \left(\frac{P_{iv',jv''}}{P_{iv'',jv'''}}\right) \tag{9}$$

Note that the ratio is independent of the experimental geometry. Using this theoretical model (corrected for the actual transmittance of the filters used) and data collected, the following results were obtained.

Reaction Cross Section

The three filters used in the experiment were the Corning CS 7-60, the Bausch and Lomb 33-78-39, and the Corning CS 7-51. Using a Cary 14, the percent transmission curves for the filters were determined, see Figure 2. The initial experiment was conducted (using the Corning CS 7-60 filter) to determine reaction cross section as a function of ions kinetic energy, see Figure 3. The collected data were normalized to a curve presented by Schlumbohm (3). With this particular filter, data were collected down to 12 eVolts. The shape of the curve below 100 eVolts is quite similar to others presented in the literature (7,3). There is agreement that the cross section decreases rapidly below about 30 eVolts. However, the same literature predicts no change in cross section above 150 eVolts. The results of this experiment are not in agreement with those findings. Instead, a gradual increase in the cross section was recorded above 200 eVolts. When the same experiment was repeated using the Bausch and Lomb filter, the increase began at about 300 eVolts. This increasing cross section continued at a fairly constant rate until the upper energy limit of the experiment, 450 eVolts. The method used to normalize the Bausch and Lomb filter data to the Corning filter data was to (1) record data at a given kinetic energy, (2) immediately change filters, and

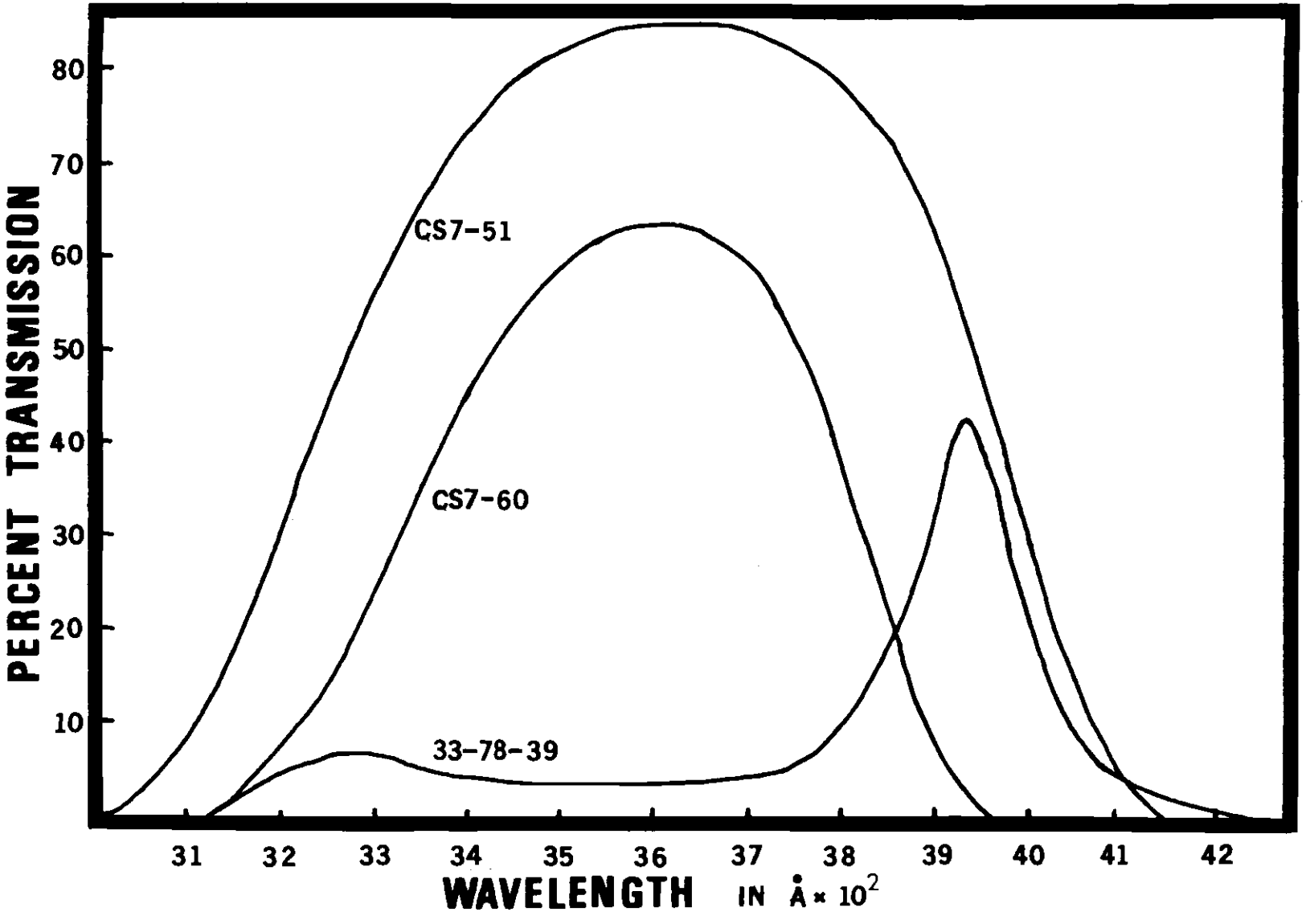

Figure 2. Percent Transmission of Experimental Filters

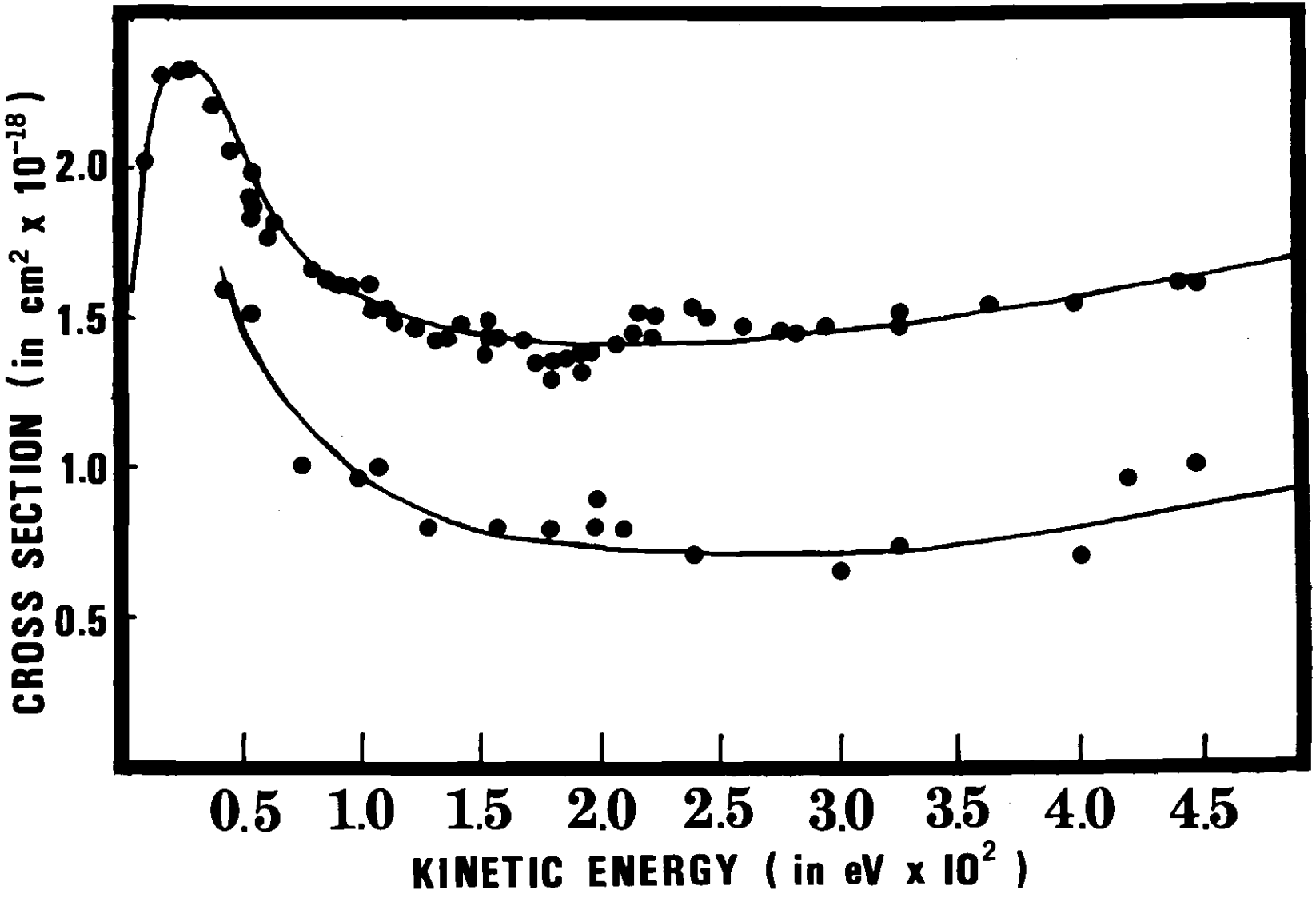

Figure 3. Kinetic Energy Dependency of the Reaction Cross Section

(3) after insuring the system was unchanged, again record data.

Relative Population Distributions

The percent transmission at each transition wavelength for each of the filters is tabulated in Table 2. From the literature it was known at what frequencies the transitions of interest occurred and what the respective Franck-Condon factors were (10,11,12). Tabulation of these data is in the appendix, Table 3.

With reference to equation (9), the only unknown left was the distribution (the ratio of intensities being determined from experimental data). To establish a distribution (at a given kinetic energy) that, when used with the theoretical model, gave the same intensity ratios as those determined experimentally took considerable time and effort. The method was as follows.

Using the Corning CS 7-60 and the Bausch and Lomb 33-78-39 filters, an intensity ratio was experimentally determined. A distribution that satisfied that ratio was then selected. Now, if the selected relative population distribution was by chance very close to the actual distribution, it should be able to be used to correctly predict intensity ratios yielded from other filters. After much time and effort, distributions were determined for two different kinetic energies, see Figures 4 and 5. Using Corning CS 7-60 and CS 7-51 filters, the experimentally determined intensity ratios were in general agreement with the predicted intensity ratios.

Table 2. The Percent Transmission at Each Transition Wavelength for the Three Filters Used in the Experiment

Transition	Wavelength in Å	Percent Transmittance		
		CS 7-60	33-78-39	CS 7-51
4,1	3076	0	0	5.5
3,0	3078	0	0	6.5
4,2	3294	22.4	6.9	54.5
3,1	3299	23.4	6.7	55.4
2,0	3309	22.5	6.5	58.2
5,4	3533	61.5	3.5	83.5
4,3	3538	62.0	3.5	83.8
3,2	3548	62.4	3.5	84.0
2,1	3564	63.0	3.5	84.5
1,0	3583	63.6	3.5	85.0
4,4	3818	33.0	12.5	77.0
3,3	3835	27.1	15.5	74.4
2,2	3858	20.0	20.0	71.5
1,1	3884	12.6	25.7	62.0
0,0	3914	5.8	37.3	57.5
6,7	4111	0	3.5	3.2
5,6	4121	0	3.1	2.3
4,5	4141	0	2.3	7
3,4	4167	0	1.5	0
2,3	4199	0	0.8	0
1,2	4237	0	0.3	0
0,1	4278	0	0	0

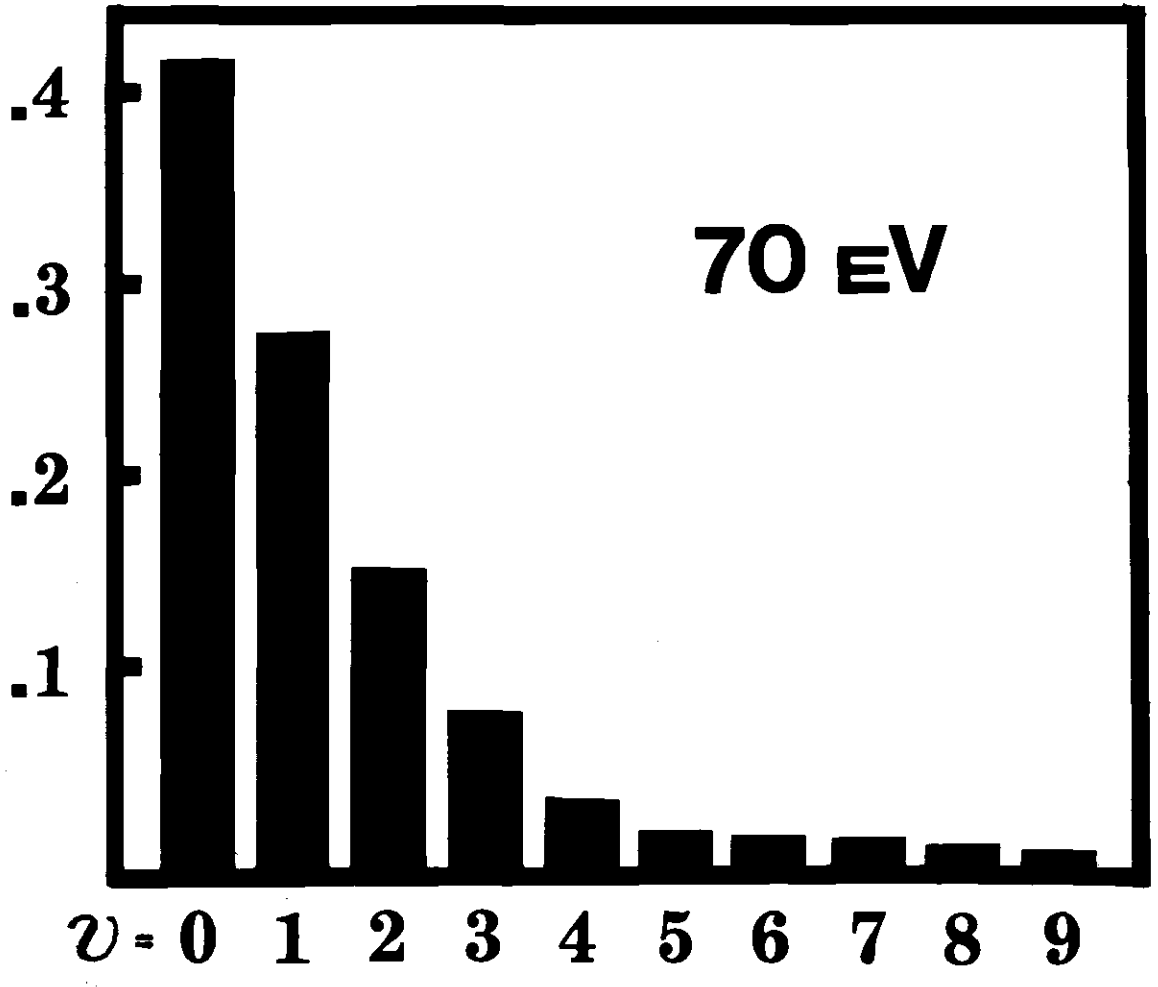

Figure 4. Relative Population Distribution of the Vibrational Quantum Levels at a Kinetic Energy of 70 eVolts

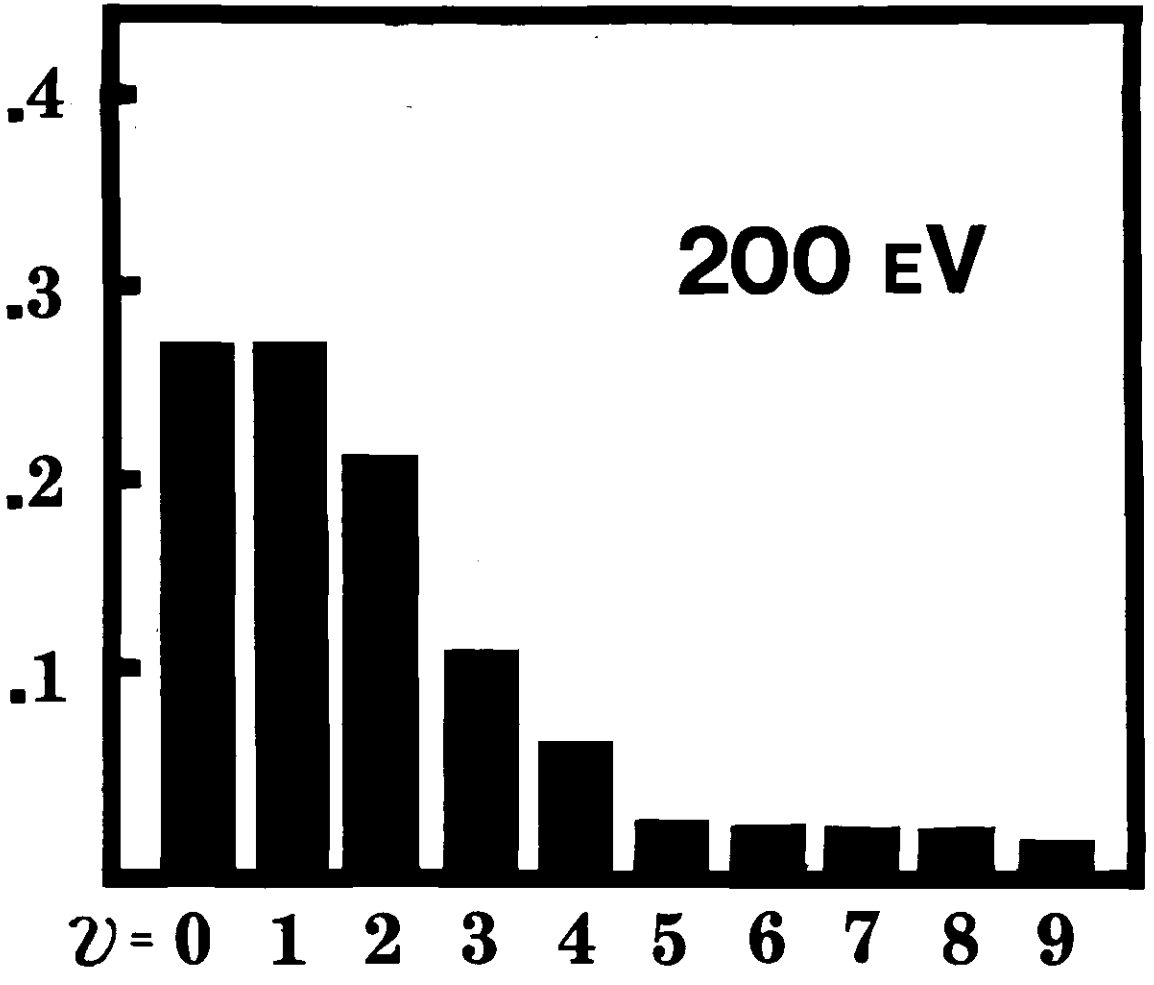

Figure 5. Relative Population Distribution of the Vibrational Quantum Levels at a Kinetic Energy of 200 eVolts

CHAPTER V

ANALYSIS AND DISCUSSION

Kinematics and Dynamics

The Ne^+ ions entering the collision region were in the ground state. Work by Hagstrum with metastable ions of the noble gases has shown that metastable states of sufficient lifetime do not exist for the neon ion (14).* When neon ions collide with neutral nitrogen molecules, approximately 80 percent of the positive ions produced are molecular N_2^+ (15). Thomas and co-workers show about 5 percent of these ions to be formed in the $B^2\Sigma_u^+$ excited state (12), whereas Philpot and Hughes believe the figure to be closer to 15 percent (16). Nevertheless, the importantly germane phenomenon to this experiment was that no transitions that cause a cascade population of the $B^2\Sigma_u^+$ excited state take place (13). Therefore, all emitted photons analyzed came only from the $N_2^+ B^2\Sigma_u^+$ species generated by collision of Ne^+ in the ground state with nitrogen gas.

Radiative lifetimes of the excited states of many species have been studied. Lawrence used an electron-excitation phase shift apparatus specifically designed to measure excited state radiative lifetimes in the approximate range of one to two hundred nanoseconds (17). This same

---

*By the use of the word "metastable," Hagstrum implies an ion which is in a very short-lived excited state and not an unstable complex ion which rapidly falls apart into one or more atomic or molecular fragments.

method was later used by Hesser who determined that, for the transition

$$B^2\Sigma_u^+ \rightarrow X^2\Sigma_g^+ \qquad \text{for } N_2^+ \text{ with } v' \text{ being } 0,$$

the radiative lifetime was $59.2 \pm 6.0 \times 10^{-9}$ sec and cascade free (18). Later work by Desesquelles, Dufay, and Poulizac gave a lifetime of $66.6 \pm 0.13 \times 10^{9}$ sec for the same transition (19). Thus, definite evidence exists to show the spontaneous radiative nature of the excited N_2^+ species generated in the collision chamber. Even if we assume a complex intermediate of the type $(N_2 \cdot Ne)^+$, it is easily shown that species excited into the $B^2\Sigma_u^+$ state could not travel out of the collision region prior to photon emission. With a 50 eVolt Ne^+ ion, the velocity and momentum at the instant of collision are in the order of 2×10^6 cm/sec and 7×10^{-17} gm-cm/sec. For a 450 eVolt ion, the values are 6×10^6 cm/sec and 21×10^{-17} gm-cm/sec. Assuming a thermal distribution of the target gas and that all kinetic energy of that gas goes into translational motion of the complex, there is still time for numerous rotations prior to the complex being able to exit the collision area without photon emission. An approximate complex velocity would be in the order of 10^6 cm/sec; the time for complex rotation, about 10^{-10} sec. Therefore, the complex travels about 10^{-4} cm for every rotation. Previous workers have shown long lived complex formation is not a significant mechanism and the reaction to be spontaneously radiative at high kinetic energies (12). Since the area seen by the photomultiplier is over 60 cm^2, there is practically no chance for an $N_2^+ B^2\Sigma_u^+$ species to exit the collision area prior to emitting a photon.

Franck-Condon Comparison

Jain and Sahni used the best available wave functions to calculate Franck-Condon factors for the ionization of N_2 (using Rydberg-Klein-Rees potential energy curves) (20). For the reaction

$$N_2(X^1\Sigma_g) - e \rightarrow N_2^+(B^2\Sigma_u^+)_{v=0,1,2,3...}$$

a specific vibrational population distribution dictated by the Franck-Condon factors will result. In other words, the ionization of N_2 gives a specific vibrational distribution in each state in which the products are formed. According to Jain and Sahni, the ionization of N_2 to the $N_2^+B^2\Sigma_u^+$ state puts about 88 percent of the species into the v=0 vibrational quantum level (20) for a Franck-Condon type transition. However, the data collected from the present experiments show only about 42 percent occupation of the v=0 level at 70 eVolts and only about 37 percent occupation at 200 eVolts. This conclusively shows that the reaction mechanism was not a Franck-Condon type transition. The Ne^+ ion beam did not ionize the nitrogen gas via the same mechanism that governed the photoionization work of Turner and May (21,22), who used monoenergetic photons to ionize molecules. In certain cases, they were so successful that vibrational structure could be resolved and used to check theoretically predicted Franck-Condon factors for accuracy. From spectral bands for the ionization of N_2 into the $N_2^+B^2\Sigma_u^+$ state, two peaks (from which Franck-Condon factors of 0.90 and 0.10 for the v=0 and v=1 transitions were elucidated) were sharply evident (21). There were in very good agreement with Jain and Sahni's theoretically predicted values of 0.89 and 0.11. Our experi-

mental values were 0.42 and 0.28 at 70 eVolts and 0.22 and 0.22 at 200 eVolts (see Figures 4 and 5) and appear to be more in agreement with a model based on a complex intermediate. Perhaps the best such model is the Phase-Space approach which will be discussed in some detail in the next section of this thesis. The values predicted by that model are .075 and .071 at 70 eVolts and .076 and .074 at 200 eVolts. The experimental results tend to favor the phase-space model.

Phase-Space Comparison

Several years ago, Light and co-workers compared results gotten from statistical phase-space calculations to averaged quantities measured in ion-molecule reactions (23). Results indicated that this theoretical approach would be useful in understanding those reactions. Fullerton and Moran later applied the statistical phase-space theory to molecular and dissociative charge-transfer reactions of the rare gases with nitrogen molecules (24). Comparisons between calculated and experimental cross sections for the molecular charge transfer channels indicated an incomplete mixing of statistically available N_2^+ product ion electronic states. Cross sections computed for endoergic dissociative channels of reaction were in good agreement with their experimental results.

Calculations of this type are based on the assumption of a "strong coupling" collision in which the probability for formation of a particular reaction channel is proportional to the ratio of phase-space available to a given product divided by the total phase-space. One rational for applying this model depends on the existence of a long-lived complex in which available energy is distributed randomly among all degrees of freedom,

another is the hardness of the collision which may be ergodic with respect to species momenta (25,26). If collision times are short, the relative positions of particles do not vary appreciably and averages over small variations in the parameters and phases may give cross sections correlating with available phase-space (24). The phase-space available for forming a given product state, i, in a given vibrational state, v_i, consistent with conservation of total energy, E_{tot} and total angular momentum, J_{tot} has been shown to be as follows (27,28).

$$\Gamma_i(E_{tot},J_{tot},v_i) = \iint \left[1 + \left(\frac{J_{rot}}{J_{tot}}\right)^2 - \left(\frac{2\,J_{z,rot}}{J_{tot}}\right)\right]^{-\frac{1}{2}} dJ_{rot}\, dJ_{z,rot} \qquad (10)$$

The limits of integration are determined by the system (29). The total energy must be conserved.

$$E_{tot} = E^o_{trans} + E^o_{vib} + E^o_{rot} = E^i_{trans} + E^i_{vib} + E^i_{rot} - Q_{oi} \qquad (11)$$

The superscripts o and i refer to the reactant and product channels, respectively, and Q_{oi} is the exothermicity of reaction. Since E^i_{trans} must be positive, the upper bound on the rotational angular momentum is given by

$$\frac{J_{rot}^2}{2I} \leqq E_{tot} - E^i_{vib} + Q_{oi} = \epsilon \qquad (12)$$

The limit on rotational energy to prevent the molecule from dissociating is

$$\frac{J_{rot}^2}{2I} < D^i_v \qquad (13)$$

where D_v^i is the dissociation energy of the diatomic molecule from the vibrational level, v.

Under the influence of the ion induced dipole potential, the requirement for product separation dictates that the final translational energy (E^i_{trans}) equal E_{final} and be equal to or greater than V(r*) where

$$V(r^*) = \frac{[E_{final}(b_{final})^2]^2}{2e^2a} \tag{14}$$

b_{final} is the product impact parameter, and a is the polarizability of the neutral species. By taking J_{orb} equal to $[\mu v_{final} b_{final}]$ and J_{tot} along the z axis,

$$J_{orb}^2 = J_{tot}^2 + J_{rot}^2 - 2(J_{tot})(J_{z,rot}) \tag{15}$$

Using equations (12) and (13)

$$E_{final} = \epsilon \left(1 - \frac{J_{rot}^2}{2I\epsilon}\right) \tag{16}$$

and the constraint on the z component of rotational angular momentum is given by the relationship

$$J_{z,rot} \geq \frac{J_{tot}^2 + J_{rot}^2 - \left[\left(8e^2a\mu^2\epsilon\right)\left(1 - \frac{J_{rot}^2}{2I\epsilon}\right)\right]^{\frac{1}{2}}}{2J_{tot}} \tag{17}$$

Using these constraints, the phase-space integral in equation (10) can be evaluated to obtain the phase-space available for forming a product diatomic stable with respect to dissociation (19,30). The total

phase-space is found by summing over all product states.

$$\Gamma(E_{tot},J_{tot}) = \sum_i \sum_v \Gamma_i (E_{tot},J_{tot},v_i) \tag{18}$$

The probability for the forming of diatomic state i in vibrational level v is

$$P(E_{tot},J_{tot},E^i_{vib}) = \frac{\Gamma_i}{\Gamma(E_{tot},J_{tot})} \tag{19}$$

where Γ_i is the phase-space for forming a stable diatomic species in state i and vibrational level v. The cross section σ is then

$$\sigma(E^o_{trans},i,v) = 2\pi \int_o^{b_{max}} P(E_{tot},J_{tot},E^o_{vib})\ b\ db \tag{20}$$

where b is the impact parameter in the reactant channel and b_{max} is the maximum impact parameter calculated from the ion induced dipole potential (31,32).

Using phase-space theory, two distributions were calculated for the reaction studied in this thesis. The computed phase-space vibrational population distributions are given in Figures 6 and 7 for the reactions of 70 and 200 volt Ne^+ ions.

Final Comments

There appears to be better agreement between the measured population distributions and those predicted using the statistical phase-space model than computed population distributions arrived at via the best

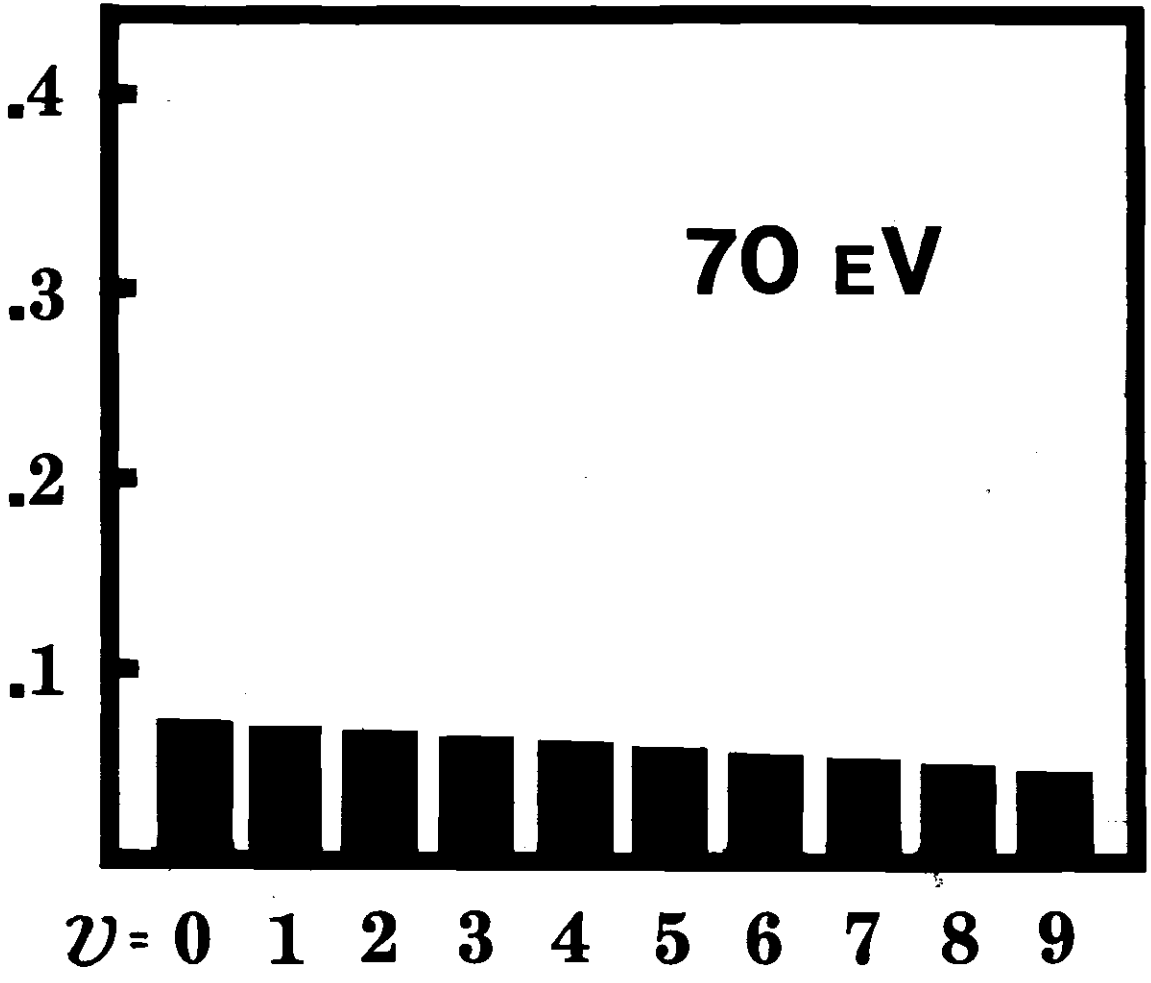

Figure 6. The Phase-Space Calculated Relative Population Distribution of the Vibrational Quantum Levels at a Kinetic Energy of 70 eVolts

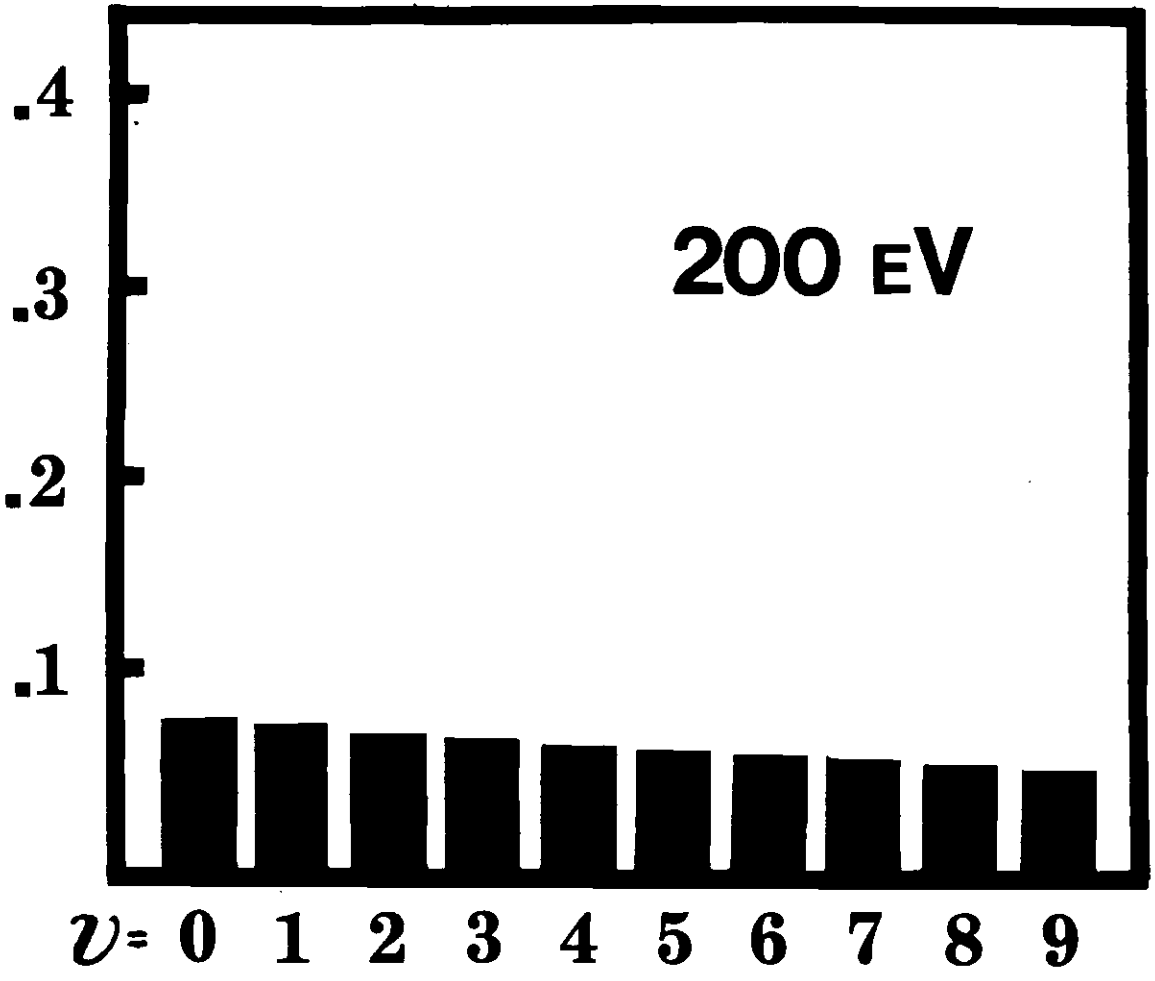

Figure 7. The Phase-Space Calculated Relative Population Distribution of the Vibrational Quantum Levels at a Kinetic Energy of 200 eVolts

available Franck-Condon factors.

It should again be pointed out that one of the assumptions used in applying the phase-space model involves the existence of a collision complex in which available energy is distributed randomly among all degrees of freedom. The alternate Franck-Condon type mechanism assumes that little perturbation of the nuclei takes place during an electron transfer reaction and that the population distribution can be computed from the overlap of the vibrational wave functions describing isolated nuclei.

It is therefore reasonable to propose that, since the measured vibrational distributions were intermediate between those predicted by the two extreme mechanisms, the reaction pathways were a combination of the two.

APPENDIX

Table 3. Wavelengths and Franck-Condon Factors for the Vibrational Transitions Associated with the Reaction $N_2^+(B^2\Sigma_u^+) \rightarrow N_2^+(X^2\Sigma_g^+) + h\nu$

Transition	Wavelength (Å)	Franck-Condon Factor
4,1	3076	.007
3,0	3078	.002
4,2	3294	.166
3,1	3299	.106
2,0	3309	.045
5,4	3533	.331
4,3	3538	.379
3,2	3548	.414
2,1	3564	.406
1,0	3583	.301
4,4	3818	.007
3,3	3835	.002
2,2	3858	.051
1,1	3884	.223
0,0	3914	.651
6,7	4111	.020
5,6	4121	.048
4,5	4141	.093
3,4	4167	.156
2,3	4199	.229
1,2	4237	.286
0,1	4278	.259

LITERATURE CITED*

1. N. G. Utterback and H. P. Broida, Phys. Rev. Lett. 15, 608 (1965).

2. M. Lipeles, R. Novick, and N. Tolk, Phys. Rev. Lett. 15, 815 (1967).

3. H. Schlumbohm, Z. Naturforsch, 23a, 970 (1968).

4. J. Van Eck, F. J. de Heer, and J. Kistemaker, Phys. Rev. 130, 656 (1963).

5. L. D. Landau, Phys. Z. Sowjetunion 2, 46 (1932).

6. H. Schlumbohm, Z. Naturforsch, 23a, 1386 (1968).

7. E. Gustafsson and E. Lindholm, Ark. Fys. (in Swedish) 18, 219 (1961).

8. R. E. Honig, J. Chem. Phys. 16, 105 (1948)

9. F. H. Field and J. L. Franklin, Electron Impact Phenomena. New York: Academic Press, 1957. p. 41.

10. R. W. Nicholls, J. Res. N'tal. Bur. Stds. 65A, 451 (1961).

11. L. Wallace, Astrophys. J. Suppl. 62, 473 (1962).

12. E. W. Thomas, G. D. Bent, and J. L. Edwards, Phys. Rev. 165, 32 (1967).

13. G. Herzberg, Spectra of Diatomic Molecules. Vol. I: Molecular Spectra and Molecular Structure. 2d ed. Princeton, N. J.: D. Van Nostrand Company, Inc., 1950.

14. H. D. Hagstrum, Phys. Rev. 104, 309 (1956).

15. E. S. Solov'ev, R. N. Il'in, V. A. Oparin, and N. V. Fedorenko, Zh. Eksperim. i Teor. Fiz. 42, 659 (1962). [English transl.: Soviet Phys.--JETP 15, 459 (1962)].

16. J. L. Philpot and R. H. Hughes, Phys. Rev. 133, A107 (1964).

*The abbreviations used herein conform to those adopted by the IUPAC and AIP as described in the List of Periodicals, Chem. Abstr. 55, 1J (1961) and later supplements.

LITERATURE CITED (Concluded)

17. G. M. Lawrence, J. Quant. Spectry. Radiative Transfer S, 359 (1965).

18. J. E. Hesser, J. Chem. Phys. 48, 2518 (1968).

19. J. Desesquelles, M. Dufay, and M. C. Poulizac, Phys. Ltrs. 27A, 96 (1968).

20. D. C. Jain and R. C. Sahni, Int. J. Quan. Chem. II, 325 (1968).

21. D. W. Turner and D. P. May, J. Chem. Phys. 45, 471 (1966).

22. D. W. Turner and D. P. May, J. Chem. Phys. 46, 1156 (1967).

23. J. C. Light, Discussions Faraday Soc. 44, 14 (1968).

24. D. C. Fullerton and T. F. Moran, J. Chem. Phys. 54, 5221 (1971).

25. J. C. Light, J. Chem. Phys. 40, 3221 (1964).

26. D. G. Truhlar and A. Kupperman, J. Phys. Chem. 73, 1722 (1969).

27. P. Pechukas and J. C. Light, J. Chem. Phys. 43, 3281 (1965).

28. J. C. Light and J. Lin, J. Chem. Phys. 43, 3209 (1965).

29. D. C. Fullerton, Thesis (Georgia Institute of Technology, 1971).

30. F. A. Wolf, J. Chem. Phys. 44, 1619 (1966).

31. G. Gioumousis and D. P. Stevenson, J. Chem. Phys. 29, 294 (1958).

32. P. Langevin, Ann. Chim. Phys. 5, 245 (1905); see E. W. McDaniel, Collision Phenomena in Ionized Gases (Wiley, New York, 1964), p. 701 for a translation of this paper.

33. H. S. W. Massey, Rept. Progr. Phys. 12, 248 (1949).